The United Nations University

GEOTHERMAL TRAINING PROGRAMME
Orkustofnun, Grensásvegur 9,
IS-108 Reykjavík, Iceland

Reports 2005
Number 23

GEOCHEMISTRY AND ISOTOPE STUDY OF THE THERMAL WATERS FROM THE URBAN GEOTHERMAL FIELD, BEIJING, CHINA

Yu Yuan
China University of Geosciences
Water Resources and Environmental Science School
29 Xueyuan Road, Haidian District
100083 Beijing
P.R. CHINA
mintyuan@126.com

ABSTRACT

The Urban geothermal field is a famous low-temperature geothermal field in China. Its production history spans more than 30 years. The geothermal system consists basically of three reservoirs, the Tieling Group (Jxt), the Wumishan Group (Jxw) and the Hongshuizhuang Group (Jxh) of the Jixian (Jx) system. Geochemical methods are used to interpret the chemical and isotopic characteristics of thermal waters in the Urban field. Because of the relatively low temperature of the thermal water, the thermal fluid does not seem to be in equilibrium with any hydrothermal minerals in the reservoir, except for chalcedony and quartz. As for mixing, the binary plot and silica-enthalpy mixing model are used, indicating that the fluids in the Urban geothermal field have been mixed with cold water. Several kinds of geothermometers are used to predict the subsurface temperatures in this area. Geothermometer calculations indicate that one can expect the highest temperature, a little over 100°C, in the centre of the sedimentary basin. Therefore, the main potential for further development of the geothermal resources is in that region. From the log (Q/K) diagram, it can be seen that the geothermal water in the Urban field has a potential for scaling. The present study indicates that the thermal water is of meteoric origin. The chemical composition of the water has changed very little during the period 1984-2000.

1. INTRODUCTION

Beijing, the capital of the Peoples Republic of China, is the political, economic and cultural centre of the nation with a population of about 12 million. It is situated on top of a large and deep sedimentary basin with an area of about 16,800 km^2, including 10,800 km^2 of a mountainous area in the north and west, and 6,000 km^2 of a plains area in the southeast (see Figure 1). Beijing has abundant geothermal resources. The area with identified geothermal potential is over 2,300 km^2. Geothermal energy plays an important role in the energy economy of Beijing City. The first geothermal observation well was drilled into a granite mass located in Fangshan County, Beijing in 1962 to a depth of 500 m, making it possible to obtain data on geothermal gradients after systematic observations of well temperatures

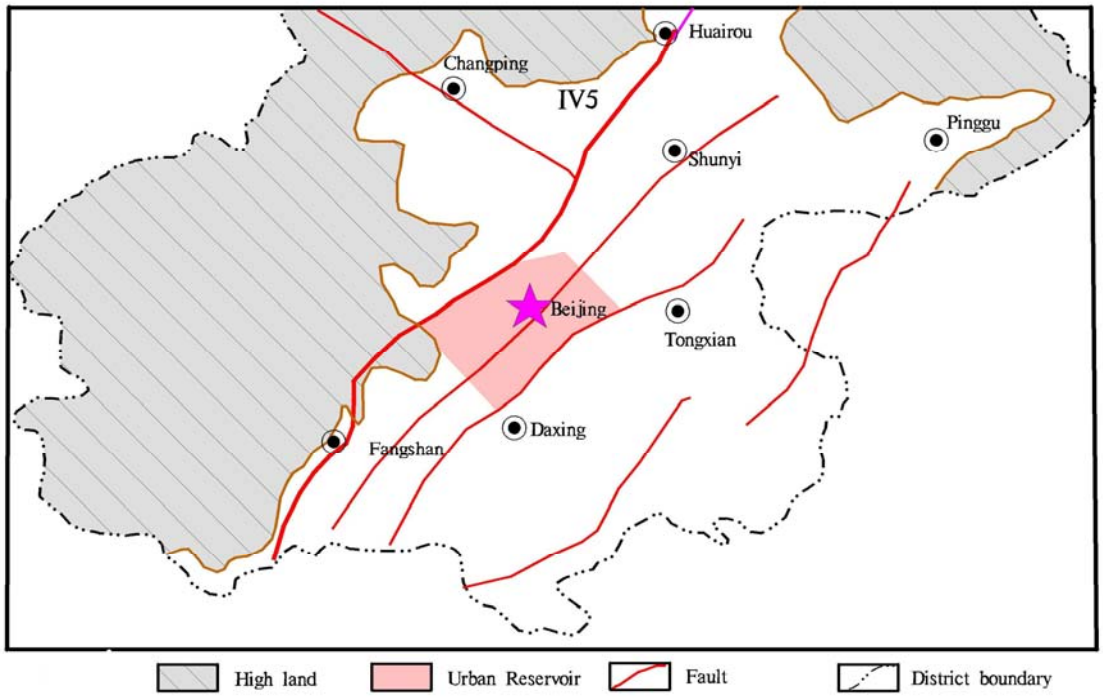

FIGURE 1: Location of the Urban geothermal field

(Huang, 2000). Now Beijing has approximately 300 production wells yielding over nine million cubic metres of hot water annually, used mainly for domestic hot water, space heating, greenhouse heating, (vegetables and flowers), bathing, balneology, aquaculture (fry hatch) and in industrial applications.

According to the geothermal planning report of 1999 (Bin et al**.,** 1999), there are 10 geothermal fields in the Beijing area (Table 1), based on the distribution of the geothermal reservoirs. Among these geothermal fields, the Urban geothermal field, lying in the central part of the city and extending over an area of 319 km^2, is one of the most important geothermal production areas, and has been utilized since the 1970s. The Urban field is a low-temperature geothermal field yielding water with a temperature in the range of 40-88°C. Its production history spans more than 30 years. The desire for developing geothermal resources has become more and more urgent especially in the last ten years, with the improvement of people's living conditions and environmental awareness. By the end of the year 2001, 82 geothermal wells had been drilled, most of them in the southeastern part of this field, of which 74 are successful. The maximum depth of the wells is 3,766 m and the highest temperature is 88°C.

TABLE 1: Geothermal fields in the area of Beijing

Geothermal field	Area (km^2)	Reservoir rock	Reservoir depth (m)	No. of wells	Water temperat. (°C)
Urban	319	Dolomite	900-3500	±70	38-88
Xiaotangshan	146	Limestone & dolomite	50-2500	±60	38-70
Tianzhu	252	Dolomite	1000-3000	15	45-89
Liangxiang	388	Dolomite	300-3500	±30	40-72
Shahe	100	Limestone & dolomite	1500-3000	13	42-72
Shuangqiao	213	Dolomite	500-1500	6	45-50
Houshayu	140	Limestone & dolomite	>2500	3	70
Lishui	202	Dolomite	400-1000	6	40-54
Yanqing	95	Dolomite	<2700	4	53-71
Fengheying	517	Sandstone, limestone & dolomite	1500-3000	1	83

With extended drilling, the proven area of the Urban field was extended from the first 100 km^2 in the southeast part of the field to the present 319 km^2. In spite of the fact that the scope of exploration and development in the field has escalated, the important part are the 120 km^2 in the southeastern part of the Urban geothermal field. Total production was nearly 4 million m^3 in 2001, mainly used for space heating, bathing, aquaculture plants and mineral water production. Long-term extraction has caused remarkable drawdown of reservoir pressure in the southern part of the geothermal field where most of the geothermal wells are located. A water level drop of up to 50 m has been observed during periods of production, and the water level has continued to decline. The annual recharge of the geothermal reservoir is about 4.0 million m^3 at the present water level.

The present study is based on the analysis of 10 fluid samples collected from different geothermal wells and some previous data on the Urban geothermal field.

2. GEOLOGICAL SETTING AND GEOTHERMAL BACKGROUND

The Beijing Urban geothermal field is a famous low-temperature geothermal field in China. The Urban field is located in a sedimentary basin bounded by a series of faults since the early Jurassic Period. These faults, trending SW-NE and NW-SE are, the main conduits of underground water and are closely related to the geothermal manifestations (Fang and Zhu, 2002). The two faults that form the northwest and southeast boundaries of the graben, Huangzhuang-Gaoliying fault and Nanyuan-Tongxian fault, are also the boundaries of the geothermal field (see Figure 2) (Liu et al., 2001). The southwest and northeast boundaries of the geothermal field are also made up of two faults, Yongdinghe fault and Jiuxianqiao fault. The Liangxiang-Qianmen fault cuts across the central part from southwest to northeast, and divides the whole area into southern and northern parts. The geothermal system in the southern part consists basically of two reservoirs made of siliceous dolomite, the Tieling group (Jxt) and the Wumishan group (Jxw). The geothermal system in the northern part is of the Wumishan group (Jxw). The two reservoirs are separated by shale (Jxh), which is about 80 m thick.

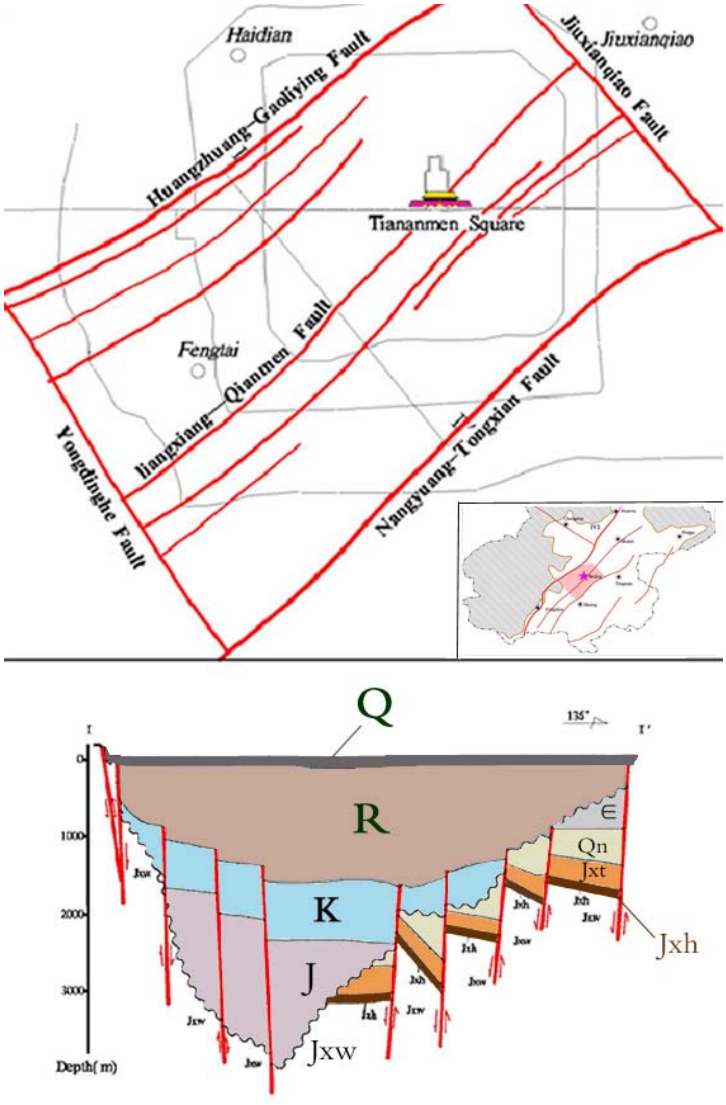

FIGURE 2: A sketch map of geological structures in the Urban field

Geothermal background and geothermal resources in the Urban field have been studied in detail by the Beijing Institute of Geological

Engineering and the China Academy of Sciences in Beijing. The main geological formations in the area include (Liu et al., 2002):

Quaternary (Q): Unconsolidated sediments;
Tertiary (R): Shale, mudstone and basalt;
Cretaceous (K): Mudstone and conglomerate;
Jurassic (J): Andesite, tuff and mudstone;
Qingbaikou (Qn): Shale, sandstone and marlstone;
Jixian (Jx): Tieling group (Jxt), dolomite; Hongshuizhuang group (Jxh), shale; Wumishan group (Jxw), dolomite.

The dolomite of the Tieling group (Jxt) and the Wumishan group (Jxw) of the Jixian system (Middle Proterozoic group), which are separated by the shale of the Hongshuizhuang group (Jxh) with a thickness of 80-90 m, is the dominant reservoir rock in the Urban field. The Tieling group (Jxt), with a thickness of 340 m, is mainly found in the southeast part of the Urban field, while the Wumishan group (Jxw) with a thickness of 2,000 m, is present all over the field. The reservoir is covered with strata of Quaternary (Q) and Tertiary (R) age in general. The conglomerate of Cretaceous (K) and lava terrane of the Jurassic (J), constitute caprocks in the central and northern parts of the field. The limestone and dolomite in the Jixian System are permeable, and constitute aquifers of cold groundwater and geothermal water. Most of the geothermal wells in the Urban field produce from these aquifers.

The thickness of the reservoir varies in different parts of the geothermal field, from about 700-1,500 m in the southeast, to more than 2,500 m in the north, about 1,500-2,500 m in the southwest, and can reach more than 3,500 m in the centre of the sedimentary basin. The geothermal gradient in the southeast part of the reservoir is often more than 3°C /100 m, but less than 2.5°C /100 m in the northern part (Liu et al., 2001).

3. CHEMICAL AND ISOTOPIC COMPOSITION OF THE THERMAL FLUID

3.1 Sampling and analysis

Geochemical studies of geothermal fluids involve three main steps: 1) sample collection, 2) chemical analysis and 3) data interpretation.

3.1.1 Sampling

Ten geothermal water samples with a temperature range of 50-90°C were collected from geothermal wells in the Urban field to analyse for isotopic composition as well as total chemical composition in June, 2004. These samples have enabled us to establish a basis for explaining the chemistry of thermal water in the Urban field.

The isotope analysis for deuterium (δD), oxygen-18 ($\delta^{18}O$) and sulfur-34 ($\delta^{34}S$) was carried out in the China Academy of Geological Sciences and the Institute of Geology, China Earthquake Administration. Analysis of the chemical composition of water samples was made by the Mineral Water Monitoring Centre, Beijing Institute of Geological Engineering. The different methods adopted are as listed in Table 2.

3.1.2 Analytical results

The results of the chemical analysis, together with the isotopic composition of water samples from geothermal wells in the Urban field are listed in Tables 3 and 4, respectively. In the Urban field, the geothermal water is generally of low mineral content, with TDS about 0.3-0.8 g/l and pH in the range

7.41-7.98; the maximum measured temperature is 89°C and the minimum 51°C. The sodium and potassium concentrations range from 25.6 to 160 mg/l and 6.47 to 18 mg/l, respectively. Some components are not listed in the following tables because their concentrations were very low, such as NO_3^-, I^- and NO_2^-. The water is colourless and odourless but contains CO_2 gas. Bicarbonate concentration is 226-330 mg/l, which is much higher than that of other anions. Calcium concentration is in the range 23-57.1 mg/l. The concentration of chloride is much lower than that of the other major anions, or in the range 9.9-97.6 mg/l. The sulphate concentration is 36.4-132 mg/l. Sodium is the main cation in most natural waters, including geothermal water, but bicarbonate is typical of cold groundwater. The source of chloride may be rainwater or evaporite deposits. Thus, the waters may be a mixture of deep circulating geothermal water and shallow cold groundwater.

TABLE 2: Most important chemical analytical methods used for the geothermal water

Composition	Method of analysis
K	Atomic absorption spectrometry
Na	Atomic absorption spectrometry
Ca	Atomic absorption spectrometry
Mg	Atomic absorption spectrometry
CO_2	Alkalinity-titration
SO_4	Ion chromatography
Cl	Ion chromatography
F	Ion selective electrode
B	Spectrophotometry
SiO_2	Spectrophotometry
Fe	Atomic absorption spectrometry
Al	Atomic absorption spectrometry
H_2S	Titration
pH	Ion selective electrode
TDS	Gravimetric
^{18}O	Mass spectrometry
D	Mass spectrometry

TABLE 3: The isotope composition of thermal water in the Urban geothermal field

Well no.	Location	Depth (m)	ΔD_{SMOW} (‰)	$\Delta^{18}O_{SMOW}$ (‰)	$\Delta^{34}S_{CDT}$ (‰)
JR-8'	Xinqiao Hotel	1401	-68.0	-10.8	27.2
JG--1	North China Optical Instrument Plant	1410	-70.0	-10.8	27.9
JR-35	Military-suppliy instrument Research Institute	1656	-70.0	-10.9	32.9
JR-45	China Healing Research Centre	2106	-75.0	-11.1	28.1
JR-59	Fengtan Baolongcheng	3609	-70.0	-10.6	27.7
JR-64	Broadcast Institute	1572	-72.0	-10.9	31.3
JR-79	Tiantan Hospital	2054	-70.0	-10.9	26.9
JR-96	Nangong Geothermal Museum	2950	-73.0	-10.5	27.3
TR-2	Yuanyuan Hotspring Hotel	1424	-69.0	-10.9	30.7
JR-119	Peking University	3168	-74.0	-11.0	21.1

3.2 Chemical features

The geochemical characteristics of thermal water depend not only on the chemical characteristics of the deep-seated geothermal water, but also on the lithology of the geothermal reservoir, movement of thermal water and replenishment of cold water. During the long period when groundwater persisted in the reservoir, inherent chemical characteristics of the geothermal water changed. The water chemistry

TABLE 4: Analytical results for major chemical components of geothermal water in the Urban geothermal field (mg/l)

Well no.	K^+	Na^+	Ca^{2+}	Mg^{2+}	NH_4^+	Fe	HCO_3	Cl^-	SO_4^{2-}	F^-	SiO_2	CO_2	Li	Sr	HBO_2	pH	Depth (m)	TDS
JR8"	11.10	81.30	53.1	20.7	0.13	1.46	268	47.0	115.0	4.80	57.4	197.7	0.164	1.67	1.2	7.69	58	603
JG1	6.47	89.80	44.1	18.2	0.16	1.46	256	45.0	107.0	6.40	44.8	189.1	0.164	1.67	1.2	7.98	52	574
JR35	17.00	160.0	45.7	15.2	0.13	0.29	330	97.6	132.0	7.20	60.0	244.6	0.164	1.67	6.2	7.44	64	805
JR45	11.60	87.60	44.1	19.1	0.17	1.94	260	44.4	106.0	6.80	50.0	190.5	0.164	1.67	1.4	7.73	57	582
JR59	10.70	56.60	52.1	20.0	0.11	1.46	226	21.1	127.0	6.50	91.3	171.8	0.164	1.67	1	7.41	88	522
JR64	8.84	139.0	23.0	14.0	0.01	0.08	287	69.8	73.9	8.00	33.0	209.2	0.164	1.67	5.6	7.87	50	624
JR79	9.09	96.20	42.1	19.4	0.08	0.76	265	53.2	104.0	4.80	45.9	193.3	0.164	1.67	1.5	7.76	52	597
JR96	9.64	59.00	57.1	20.4	0.04	0.42	242	21.7	128.0	5.80	55.5	175	0.164	1.67	0.4	7.94	70	545
TR2	18.00	138.0	46.1	18.8	0.08	0.14	305	80.9	126.0	6.70	43.4	224.4	0.164	1.67	5	7.53	51	740
JR119	7.11	25.60	46.1	16.4	0.26	2.20	226	9.9	36.4	6.50	54.1	165	0.164	1.67	0.4	7.97	59	377

can be used to determine underground temperatures as well as boiling and mixing relationships during geothermal exploration (Tonani 1980).

The chemical composition of the thermal fluids can be used to identify the nature of the geothermal system.

3.2.1 Cl-SO_4-HCO_3 triangular diagram

In order to classify the waters, the Cl-SO_4-HCO_3 triangular diagram (Giggenbach, 1991) is often used. It helps to discern immature unstable waters and give an initial indication of mixing relationships or geographical groupings. The diagram shows several types of thermal water (including immature waters, peripheral waters, volcanic waters and steam-heated waters). It gives a preliminary statistical evaluation of groupings and trends. The position of a sample point is ascertained by obtaining the sum (S) of the concentrations (C) of the three constituents considered (Giggenbach, 1991):

$$S = C_{Cl} + C_{SO4} + C_{HCO3}$$

and then calculating the % of the three anions (Cl, SO_4 and HCO_3):

$$Cl(\%) = \frac{100C_{Cl}}{S};\quad SO_4(\%) = \frac{100C_{SO4}}{S};$$

$$HCO_3(\%) = \frac{100C_{HCO3}}{S}$$

The relative Cl, SO_4 and HCO_3 contents of the water samples are plotted on the triangular Cl-SO_4-HCO_3 diagram.

Figure 3 shows that most of the geothermal waters in the Urban field are close to the bicarbonate corner, being bicarbonate-rich waters with a neutral pH. The reservoir rocks in the Urban field are composed of dolomite. Waters emerging from such reservoirs is naturally rich in calcium and bicarbonate ions as is the water studied. The concentration of sulphate in the thermal water is also rather high. That indicates that the relative abundance of SO_4 and HCO_3 in the Urban field water in relation to Cl, is a reflection of a peripheral nature of the thermal water in the Urban field. Figure 3 suggests that it is not suitable for the use of geoindicators.

3.2.2 Na-K-Mg triangular diagram

The Na-K-Mg triangular diagram (Giggenbach et al., 1983) can be used to classify waters into full equilibrium, partial equilibrium and immature waters (dissolution of rock with little or no chemical equilibrium). The diagram can be used to better clarify the origin of the waters, and then determine whether the fluid has equilibrated with hydrothermal minerals and to predict the equilibration temperatures, $T_{Na\text{-}K}$ and $T_{K\text{-}Mg}$. The diagram is based on the temperature dependence of the three reactions:

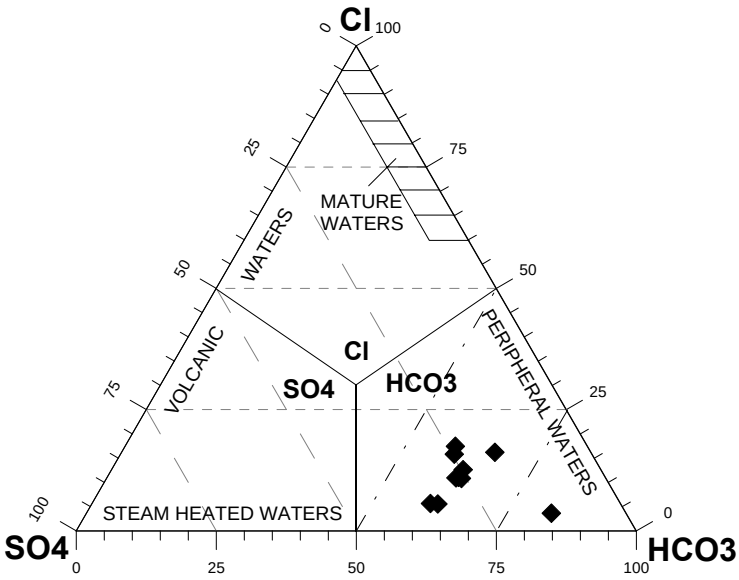

FIGURE 3: Cl-SO_4-HCO_3 ternary diagram used for the classification of water samples from the Urban field

$$K-feldspar + Na^{+} = Na-feldspar + K^{+}$$

$$2\,albite + 0.8\,K-feldspar + 1.6\,water + Mg^{2+} = 0.8\,Mica + 0.2\,chlorite + 5.4\,silica + 2\,Na^{+}$$

$$2.8K-feldspar + 1.6\,water + Mg^{2+} = 0.8\,Mica + 0.2\,chlorite - 5.4 silica + 2\,K^{2+}$$

A large number of samples can be plotted simultaneously on this diagram, and mixing trends and grouping predicted. The sum is calculated as:

$$S = \frac{C_{Na}}{1000} + \frac{C_K}{100} + \sqrt{C_{Mg}}$$

Then the "%*Na*", "%*K*" and "%*Mg*", can be calculated as;

$$\%Na = \frac{C_{Na}}{10S}; \quad \%K = \frac{C_K}{S};$$

$$\text{and} \quad \%Mg = 100\frac{\sqrt{C_{Mg}}}{S}$$

where *C* is in mg/l

Evaluation of analytical data of Na, K and Mg contents, using Figure 4, allows a clear distinction to be made between waters suitable or unsuitable for the application of ionic solute geothermometers. Because of the low temperature and the high Mg concentration, all the water sample points plot very close to the Mg corner in this diagram. It suggests that the geothermal water in the Urban field may be mixed with cold

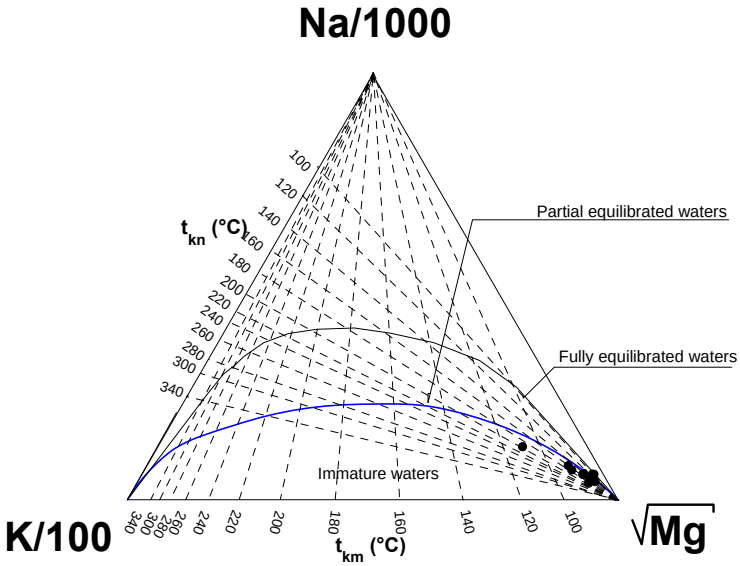

FIGURE 4: The Na-K-Mg equilibrium diagram for water samples from the Urban field

groundwater. The relatively high Mg concentration is due to the bicarbonate type of the geothermal water. Data points in this area may then be taken to correspond to those of "immature" waters generally, to waters unsuitable for the evaluation of Na/K-equilibration temperatures. Therefore, cation geothermometry is not likely to yield reasonable equilibration temperatures. The best option is therefore to use silica geothermometers in the Urban field.

3.2.3 Piper diagram

A Piper diagram is a form of the trilinear diagram. In the Piper diagram the major ion concentrations are plotted as percentages of milli-equivalents in two base triangles. The total cation and the total anion concentrations are set equal to 100% and the data points in the two triangles are projected onto an adjacent grid. This plot reveals useful properties and relationships for large sample groups. The main purpose of the Piper diagram is to show clustering of data points to indicate samples that have similar compositions. All major elements can be displayed in the Piper diagram. However, it only displays relative ratios rather than absolute concentrations. All samples in an open database or selected sample groups can be plotted in a Piper diagram.

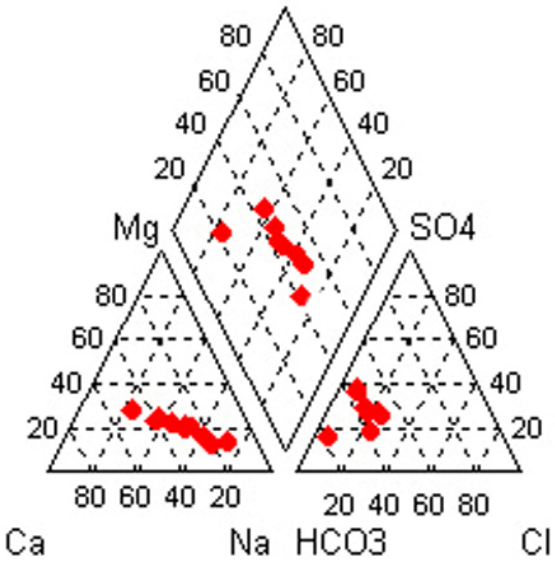

FIGURE 5: Piper diagram showing chemical types of geothermal water in the Urban field

The main chemical type of geothermal water within the northwest part of Yanqing is SO_4-Na, while Na-Cl or HCO_3-SO_4-Na-Ca is the type in the depressed area of the southeasternmost part of Fengheying. Actually, there are minor differences in the chemical type of geothermal water in the plains area, which can be detected in a Piper diagram (Figure 5). Table 5 shows the chemical characteristics of geothermal waters in the Urban field. The chemical type of geothermal waters in the Urban field can be deduced from the diagram. The dominant cations are sodium and calcium. Sodium is also characteristic of underground geothermal water, while the dominant anion is bicarbonate (Zheng, 2000). So the geothermal water in the Urban field can be classified as bicarbonate-sodium-chloride, although there are slight differences between individual waters.

TABLE 5: Chemical characteristics of geothermal waters in the Urban field

Well no.	Geothermal water type
JR8'	Na-Ca-Mg-HCO_3-SO_4
JG1	Na-Ca-HCO_3-SO_4
JR35	Na-Ca-HCO_3-Cl-SO_4
JR45	Na-Ca-HCO_3-SO_4
JR59	Na-Ca-HCO_3-SO_4
JR64	Na-HCO_3-Cl
JR79	Na-Ca-HCO_3-SO_4
JR96	Ca- Na-Mg-HCO_3-SO_4
TR2	Ca- Mg-Na-HCO_3
JR119	Na-Ca-HCO_3-SO_4-Cl

3.2.4 Schoeller diagrams

The Schoeller diagram can be used to demonstrate hydrochemical changes with time or between different locations. The values for log concentration of constituents from a number of water samples are connected with a line. Because logarithmic values are used, a wide range of concentrations can be shown. The effect of mixing with dilute water (as well as gain or loss of steam) has the effect of moving the connecting line vertically without changing its shape (Truesdell, 1991). Different water types are displayed by crossing lines.

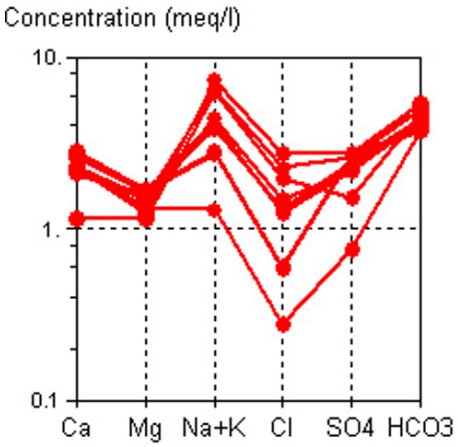

FIGURE 6: Schoeller diagram for geothermal water in the Urban field

The alignment of the ions in the water samples from the Urban field have been cross-plotted in a semilogarithmic Schoeller plot (Figure 6). It can be seen from the plots that the ten geothermal water samples have a similar composition with some minor differences. The concentrations of some constituents such as Ca, HCO_3 and K are relatively high. The diagram also shows that the geothermal water has passed through similar rock types, so it confirms that the water comes from the same lithology and similar aquifers (Connolly et al., 1990).

3.3 Isotopic composition

Stable isotopes are a powerful tool for determining origin and direction of fluid migration. The intensity of the interaction between the fluids and the minerals in rocks can be assessed. Many fluid-driven processes are characterized by the degree to which fluid flow is concentrated into zones of high permeability. The origin of fluid and its salinity are an integral part of geothermal resource exploration and development (Árnason 1976).

The stable isotopes of hydrogen and oxygen in geothermal water are usually used to obtain more reliable information about the origin and the possible recharge to an aquifer. Deuterium is used as a natural tracer to locate the catchment area of a geothermal reservoir and to investigate the flowpaths of the regional groundwater, while the ^{18}O shift for each system gives information about water-rock interaction at depth. Low-temperature geothermal water can be regarded as a "mixed average sample" for precipitation during a certain period. The isotope ratios in precipitation are controlled by the local latitude, altitude, temperature and season (Yao, 2000). For the Urban field, which is a relatively small geographical unit, the effects of latitude, altitude and season can be regarded as approximately homogeneous. Therefore, the reason for isotopic differences from place to place may be the variation in temperature and precipitation during a certain period. The Global Meteoric Water Line (GMWL) (Craig, 1961) plot is the standard way to portray data on stable isotopes from water. It is defined by the equation $\delta D = 8 \times \delta^{18}O + 10$. Most precipitation and groundwater plot close to this line. Most of the present water samples plot on the Global Meteoric Water Line.

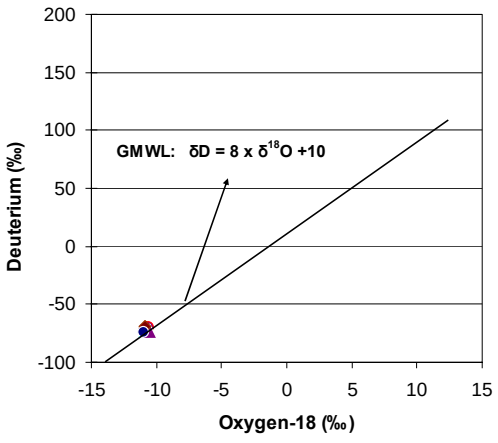

FIGURE 7: $\delta^{18}O$ vs. δD for the geothermal water in the Urban field

The water samples were analysed for the isotope ratios $\delta^{34}S$, $\delta^{18}O$, $\delta^{13}C$ and δD (see Table 3). Figure 7 shows the relationship between $\delta^{18}O$, ranging from -11.1 to -

10.5‰, and δD, ranging from -75 to -68‰. All the data points plot close to the Global Meteoric Water Line, indicating that the geothermal waters in the Urban field are mainly fed by meteoric water, through a long period of circulation of rainwater precipitation.

The thermal waters are enriched both in O-18 and deuterium isotopes. Interaction of the thermal waters with the surrounding rocks is evident in the temperature relationship for the isotopes (Hitchon and Friedman, 1969). In the Tertiary aquifers, deuterium varies slightly with temperature, while O-18 is enriched with increasing temperature (Figures 8 and 9). This implies that the interaction between water and rock is affected by temperature and that this has produced a strong O-18 shift in the Tertiary aquifers. Because of low salinity, geothermal water leaches the rock matrix. This is one of the reasons why deuterium is less affected than O-18 during this process (Pang 2000).

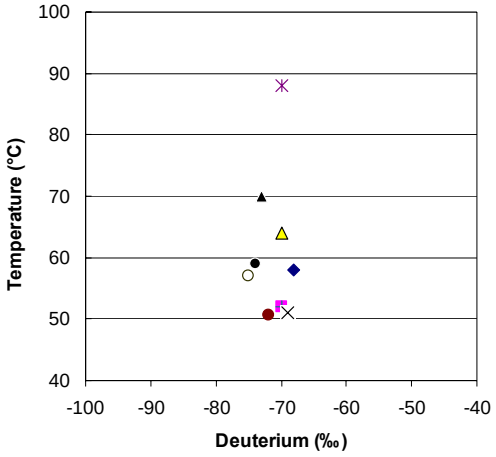

FIGURE 8: δD vs. temperature for the geothermal water in the Urban field

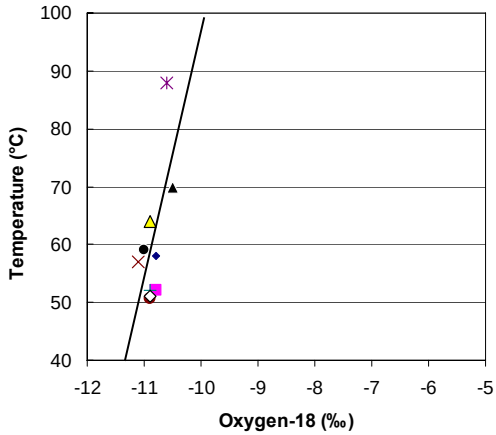

FIGURE 9: $\delta^{18}O$ vs. temperature for the geothermal water in the Urban field

3.4 Scale prediction

Scaling problems are common during the utilization of geothermal water. Scaling takes place in production wells, pipelines and other surface equipment and largely restricts the utilization efficiency of geothermal energy. The extent of scaling from geothermal water in a pipeline is mostly dependent on those constituents that may form insoluble compounds that precipitate as scales. In water of the type considered here these would be silica, calcium, magnesium and carbonate. Scales that might form include silica, calcite and magnesium silicates. Types of water and temperature changes can also affect scaling. Silica and calcite are two well-known forms of deposits that are difficult to remove from geothermal production equipment. The amount of silica dissolved in the geothermal water depends on the solubility of quartz in geothermal reservoirs. However, amorphous silica is the form which precipitates from geothermal fluids upon concentration and cooling. Silica deposition and scaling will take place in geothermal wells and surface facilities when the concentration of silica exceeds the solubility of amorphous silica. Therefore, reliable analysis and simulation of the thermal fluid changes during utilization are needed to predict scaling potential.

The program WATCH (Arnórsson et al., 1982, 1983; Bjarnason, 1994) was used to calculate the relationship between the chemistry of the deep circulating water and the solubility of minerals and to evaluate the state of calcite and amorphous silica saturation of the aquifer water at selected temperatures. The scaling potential is evaluated by computing log (Q/K), where Q means the calculated ion activity product corresponding to different minerals in the geothermal water and K is the theoretical solubility constant for the respective minerals at a certain temperature. If the calculated value for a mineral is equal to its theoretical value, log (Q/K) = 0. This means that the deep water in the reservoir has reached equilibrium with this mineral. If the value is above zero, it shows supersaturation, but below zero, it indicates undersaturation. If some minerals are close to equilibrium at a certain temperature, it means that these minerals have equilibrated with the water at that temperature, and the temperature represents the reservoir temperature.

Ten thermal water samples from different geothermal wells were selected to carry out the equilibrium calculation with the program WATCH in the temperature range 40-120°C. Seven types of minerals were chosen to ascertain the equilibrium state. They are fluorite, quartz, anhydrite, chrysotile, chalcedony, amorphous silica and calcite. The mineral equilibrium diagrams for the selected wells are presented in Figure 10. All these diagrams appear to have a similar pattern. In the diagrams for JG1, JR96 and JR119, the thermal water is supersaturated with respect to chrysotile. The log (Q/K) for chrysotile and chalcedony intersect the log (Q/K) = 0 line close to the measured temperature of 64°C in the diagram for JR35. All the samples are slightly undersaturated with respect to anhydrite and amorphous silica over the reference temperature range, and they cannot possibly be precipitated. The whole system is in equilibrium with chalcedony and quartz at the discharge temperature and the two minerals plot close to the saturation line. All these geothermal waters are supersaturated with respect to calcite at all reference temperatures. The diagrams show that log (Q/K) for calcite has an upward tendency; for most of the samples it exceeds 1 at the measured temperature, and calcite is thus considered to be very likely to cause scaling. Chrysotile also has an obvious upward shift; potential scaling could be expected. If the temperature of the geothermal water were to increase, the thermal water would still remain supersaturated with respect to calcite and chrysotile. These results agree with field observations.

3.5 Chemical geothermometry

Chemical geothermometry is used to evaluate the reservoir temperature and predict possible cooling in the reservoir during production. There are two general types of geothermometers: 1) those which are based on absolute concentrations of a constituent in solution, such as silica geothermometers, and 2) those which are based on ratios of two or more constituents in solution (Arnórsson 2000). Whether geothermometers work well at high or low temperatures is a function of the temperature dependence of the reactions and the rate of the reaction at different temperatures. In fact, silica temperature is more reliable at low temperatures than Na-K temperature. Some chemical geothermometers have been calibrated by laboratory experiments, whereas others are empirical relations deduced from many fluid samples, maybe unsuitable for waters in different areas (Arnórsson 1975). Most geothermometers give temperatures in good accordance with measured temperatures. However, fluids sampled at the surface are often not appropriate for determining the geothermal system source temperature with geothermometers because of changes in water chemistry at shallow depths.

3.5.1 Silica geothermometers

Calculation of temperature using silica geothermometers is based on the fact that the concentration of silica in water solutions is determined by the solubility of silica at the temperature of water-rock interaction (Fournier and Rowe 1966). The solubility of silica rises steeply between 100 and 300°C. Since precipitation is quite slow with decreased temperature, the silica concentration found in surface water is a good indicator of the subsurface reservoir temperature. The total silica concentration is a function of temperature. Different equations have been suggested for the approximation of this functional dependence obtained on the basis of mathematical processing of laboratory experimental data and data on measurements of temperature and silica concentrations in water from wells in geothermal systems.

The increased solubility of quartz at elevated temperatures has been used extensively as an indicator of geothermal temperatures (Fournier and Potter, 1982). In systems with temperature above about 180-190°C, equilibrium with quartz has been found to control the silica concentration, whereas at lower temperatures, chalcedony maybe the controlling phase. Temperature can be derived from the following relationships for equilibrium with these silica polymorphs from 0-250°C, where SiO_2 concentrations are in ppm:

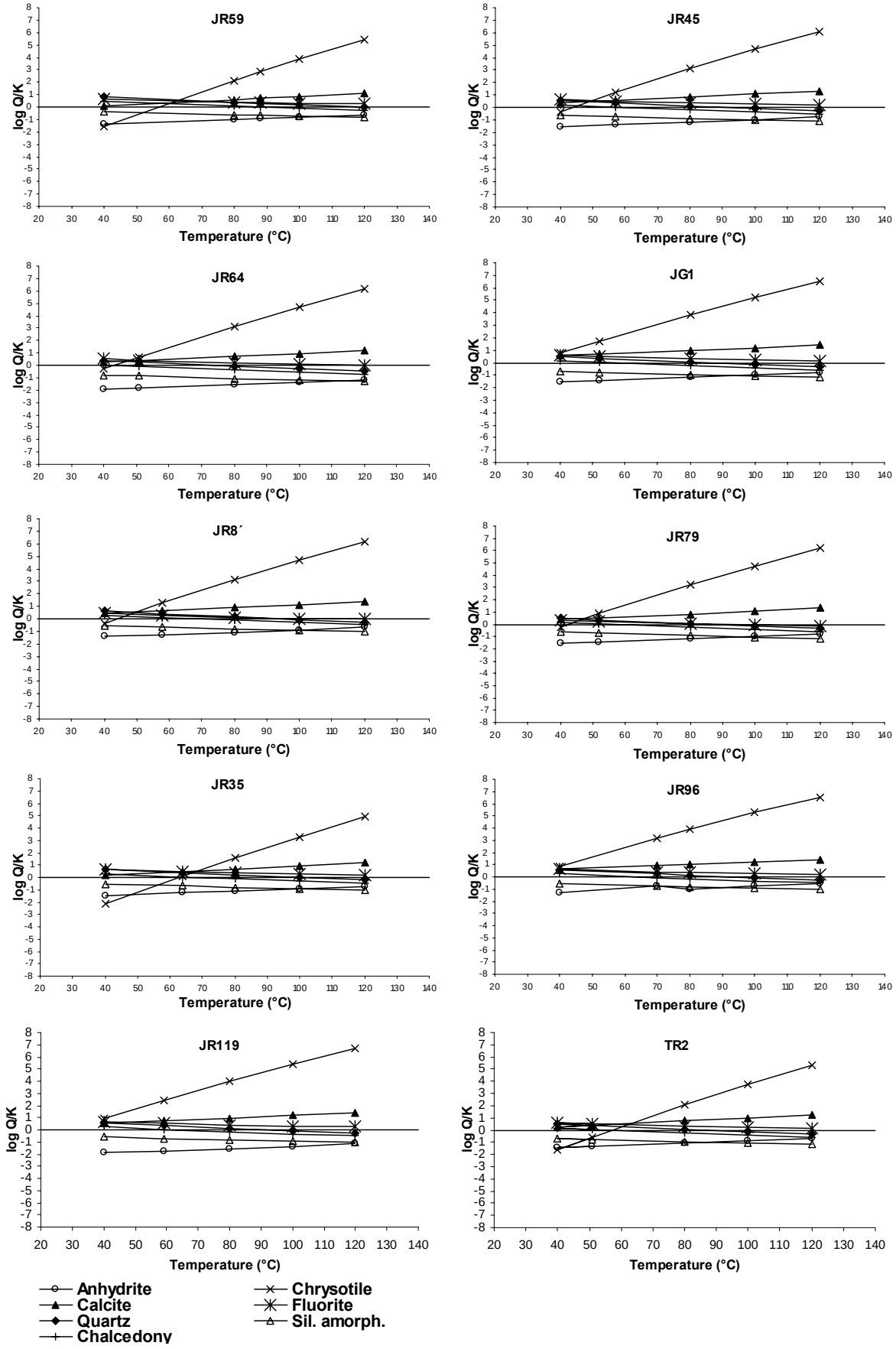

FIGURE 10: Log (Q/K) diagrams for thermal water samples from the Urban field

Quartz temperature (Fournier and Potter, 1982):

$$T°C = -42.198 + 0.28831 SiO_2 - 3.6686 \times 10^{-7} SiO_2^{\ 3} + 77.034 \log SiO_2$$

Quartz - no steam loss (Fournier, 1977):

$$T°C = \frac{1309}{5.19 - \log SiO_2} - 273.15$$

Quartz - max steam loss at 100°C (Fournier, 1977):

$$T°C = \frac{1522}{5.75 - \log SiO_2} - 273.15$$

Chalcedony- no steam loss (Fournier, 1977):

$$T°C = \frac{1032}{4.69 - \log SiO_2} - 273.15$$

Chalcedony – max steam loss at 100°C (Fournier, 1977):

$$T°C = \frac{1182}{5.09 - \log SiO_2} - 273.15$$

Chalcedony - no steam loss (Arnórsson et al., 1983):

$$T°C = \frac{1112}{4.91 - \log SiO_2} - 273.15$$

Chalcedony – max steam loss at 100°C (Arnórsson et al., 1983):

$$T°C = \frac{1264}{5.31 - \log SiO_2} - 273.15$$

3.5.2 Cation geothermometers

The Na-K-Ca geothermometer was developed by Fournier and Truesdell (1973), using an empirical relation between relative concentrations of these elements in surface water and reservoir temperatures, assuming the base exchange reaction at temperatures above 100°C. The relationships of Na^+, K^+ and Ca^{2+} are explained in terms of Ca^{2+} participating in aluminium silicate reactions, and the amounts of dissolved Na and K are therefore influenced by the dissolved Ca, even though the final amount of aqueous Ca may be controlled largely by carbonate solubility and carbon dioxide (Nicholson, 1988).

The calculated temperature using the Na-K-Ca-geothermometer is found using the following equation:

Na-K-Ca temperature (Fournier and Truesdell, 1973):

$$T°C = \frac{1647}{\log(\frac{C_{Na}}{C_K}) + \beta\left[\log(\frac{\sqrt{C_{Ca}}}{C_{Na}}) + 2.06\right] + 2.47} - 273.15$$

C_{Na}, C_K, C_{Ca} are concentrations of sodium, potassium, and calcium cations, correspondingly expressed in mole/l, where β is a coefficient with the following values:

β =1/3, if the value of ($\beta \log(\frac{\sqrt{C_{Ca}}}{C_{Na}})$ +2.0) is negative, or T >100°C,

β =4/3, if the value of ($\beta \log(\frac{\sqrt{C_{Ca}}}{C_{Na}})$ +2.0) is positive, or T <100°C.

The Na-K geothermometer is based on theoretical thermodynamic considerations. It provides additional hints on the "thermal history" of the geothermal fluid during a long period of ascent. The quartz geothermometer responds relatively fast to changes in temperature. The Na-K geothermometer, on the other hand, is much slower to respond and often keeps a record of "old temperatures". Many Na-K temperature functions have been presented by different authors. The following equations are some of them. The concentrations of Na and K are in mg/kg.

Na-K temperature (Arnórsson et al., 1983):

$$T°C = \frac{933}{0.993 + \log(\frac{Na}{K})} - 273.15$$

Na-K temperature (Giggenbach, 1988):

$$T°C = \frac{1390}{1.75 + \log(\frac{Na}{K})} - 273.15$$

Na-K temperature (Truesdell, 1976):

$$T°C = \frac{856}{0.857 + \log\left(\frac{Na}{K}\right)} - 273.15$$

Na-K temperature (Tonani, 1980):

$$T°C = \frac{833}{0.780 + \log\left(\frac{Na}{K}\right)} - 273.15$$

The *K-Mg geothermometer* responds much faster to a change in temperature, so it can be used to estimate the most recent temperature in a geothermal reservoir. It is based on the equilibrium between water and the mineral assemblage K feldspar, K-mica and chlorite in rock.

K-Mg temperature (Giggenbach, 1988):

$$T°C = \frac{4410}{14.0 - \log(\frac{K^2}{Mg})} - 273.15$$

In addition to Na-K, K-Mg and Na-K-Ca geothermometers, the *ratios Li/Mg* and *Li/Na* and the $^{34}S/^{32}S$ *isotopes* are among those that have been applied as geothermometers to geothermal waters.

The chemical geothermometer results calculated by the WATCH program (Arnórsson et al., 1982, 1983; Bjarnason, 1994) for the thermal waters in the Urban field are presented in Table 6. The ionic balances for the water samples gave results ranging from -3.53 to +2.67, which is acceptable and the data can be used for detailed interpretation. The wellhead temperatures measured for the geothermal wells are mostly in the range 50.7-88°C. Silica in all geothermal waters in the Urban field is in equilibrium with respect to chalcedony, thus it is possible to calculate the reservoir temperature using the chalcedony geothermometer. It can be seen from the data listed in Table 6 that the reservoir temperatures indicated by the calculated chalcedony temperature are much closer to the measured temperature of the geothermal wells than values calculated by the other geothermometers. Generally, the quartz temperature calculated by the silica geothermometer is 10-20°C higher than the measured wellhead temperature. The quartz temperature in the Urban field is found to be about 83-131°C or 20-30°C higher than the measured wellhead temperature. The results of geothermometer calculations as well as data on mineral-solution equilibria prove that the chalcedony geothermometer is more suitable than the quartz geothermometer for estimating reservoir temperatures in the Urban field. Chalcedony controls dissolved silica in the reservoir of the field. The chalcedony geothermometer temperature for wells JR35 and JR59, which are close to the centre of the sedimentatary basin, are 80.4 and 103.8°C, respectively, higher than for other geothermal wells within the Urban field. It indicates that the highest temperature in the Urban field is found in the centre of the sedimentary basin, the location of maximum depth to the caprock. There is a good potential for developing the geothermal resources in that region.

Because the geothermal waters of the Urban field are immature waters (see Figure 4), the Na-K geothermometer cannot be applied to the Urban field. The temperatures based on the Na-K geothermometer range from 156 to 313°C (see Table 6), too high with respect to other information on the reservoir, while the tempeatures based on the K-Mg geothermometer range from 61 to 119°C, close to the measured temperatures.

TABLE 6: Geothermometer temperatures for the thermal waters in the Urban field

No.	Well no.	Measured temperat. (°C)	SiO_2 (mg/l)	Ionic balance	Quartz temp. (°C)	Chalcedony temp. (°C)	K-Mg temp. (°C)	Na-K temp. (°C)
1	JR8´	58.0	57.4	-0.96	96	65	74	236
2	JR45	57.0	50.0	-0.66	101	71	71	232
3	JR64	50.7	33.0	-0.06	83	51	75	156
4	JR79	52.0	45.9	-0.5	98	67	82	196
5	JR96	70.0	55.5	-2.47	106	76	80	255
6	JR119	59.0	54.1	-1.42	105	74	96	313
7	TR2	51.0	43.4	2.67	95	64	61	231
8	JR35	64.0	60.0	-0.92	110	81	61	208
9	JG1	52.0	44.8	-3.54	85	53	119	168
10	JR59	88.0	91.3	-2.48	131	104	75	271

3.6 Mixing models

Mixing of thermal water with cold groundwater in shallow parts of hydrothermal systems appears to be common. The use of chemical and isotopic geothermometers to estimate subsurface temperatures from the composition of surface discharges is based on the fact that dissolved constituents are in equilibrium in geothermal fluids which may cool during upflow either conductively or by boiling due to depressurization, or by both processes; and different geothermometers will be affected differently (Arnórsson 1985). Some indications of mixing discussed by Fournier (1979) are as follows:

1. Variations in chloride concentration of boiling springs too great to be explained by steam loss;
2. Variations in ratios of relatively conservative elements that do not precipitate from solution during movement of water through rock, such as B/Cl;
3. Variations in oxygen and hydrogen isotopes (especially tritium);
4. Cool springs with large mass flowrates and much higher temperatures indicated by chemical geothermometers (difference greater than 50ºC); and
5. Systematic variations of spring composition and measured temperatures.

3.6.1 Binary plot diagram

Mixing of geothermal and cold water and the subsequent application of mixing models to estimate subsurface temperatures in geothermal systems depends on the mixing of two components of quite different composition in such a way that the concentrations of reactive components do not change much after mixing has taken place. Mixing of this kind is likely to be confined to upflow zones. Mixing at deep levels in geothermal reservoirs is likely to be completely masked for reactive constituents through re-equilibration of these constituents subsequent to mixing (Arnórsson, 1991). Mixing of two kinds of waters can be shown on a plot of one conservative species against another. Binary plots of Cl vs. Na, K, Ca and B; SO_4 vs. Ca; and SiO_2 vs. Cl, are presented in Figure 11.

Cl is a conservative component in geothermal fluids. The concentration of Cl will increase continuously during progressive rock dissolution. In Figure 11, the Na values are directly proportional to the Cl content. Similar linear relationships are found for B, Cl and Ca and SO_4, although the values for B and Ca are somewhat dispersed with respect to Cl and SO_4, respectively. No obvious relationship is observed between Ca and K vs. Cl and Cl vs. SiO_2.

3.6.2 Silica mixing model

In order to estimate reservoir temperature, the silica enthalpy mixing model (Fournier, 1977) was also used for comparison and further classification. The cold water point is assumed to represent the hypothetical cold water (e.g. temperature, T = 10ºC, and silica, SiO_2 = 20 ppm) in the study area (Stanasel and Ludovic, 2003). A straight line drawn from a point representing the non-thermal component of the mixed water (Figure 12) through the mixed-thermal water to the intersection with the quartz solubility curve gives the initial silica concentration and enthalpy of the hot-water component. This procedure assumes that any steam formed adiabatically (as the hot-water component moved up to a more shallow environment), did not separate from the residual liquid water before mixing with the cold-water component.

Based on the silica-enthalpy mixing model (Figure 12), three lines can be obtained. The upper line joining the cold water point, sample 1 (JR8´) and sample 10 (JR59), intersects the quartz solubility curve, and the predicted temperature is 180.5ºC. The medium line connects the cold water point, sample 5 (JR96) and sample 9 (JG1) and gives the reservoir temperature as 150ºC. The lowest line connects through the cold water point, sample 2 (JR45), sample 6 (JR119) and sample 8 (JR35), and the subsurface temperature of 160ºC is obtained. These predicted temperatures are higher than the reservoir temperatures obtained by the geothermometers (Table 6), indicating that most of the geothermal fluids have probably mixed with cooler water in the reservoir.

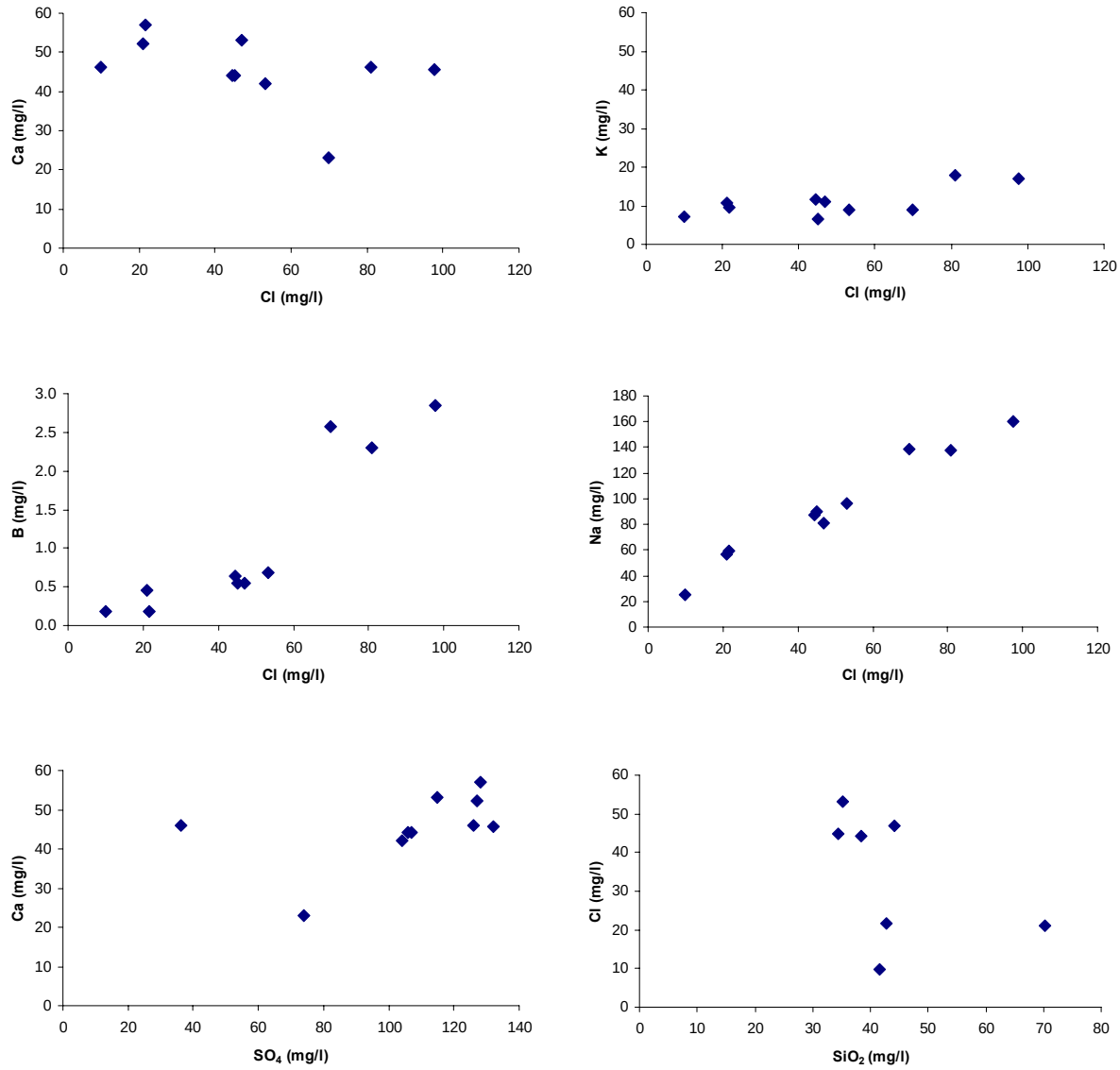

FIGURE 11: Binary plots of Cl vs. cations and B, SiO_2 vs. Cl and Ca vs. SO_4 for water samples

4. GEOTHERMAL DEVELOPMENT AND UTILIZATION

4.1 Geothermal development

Large-scale geothermal use in the Beijing Urban field started in 1971, with the successful completion of the first geothermal well (Liu et al., 2002). The amount of production was increased steadily for many years, and the annual production reached the highest in its history, more than 5 million m^3 in 1985 (see Figure 13). More than 90% of the 82 production wells drilled up to 2001 are located in the southeast part of the geothermal field. The depth of the wells is in many cases less than 2,000 m. Since

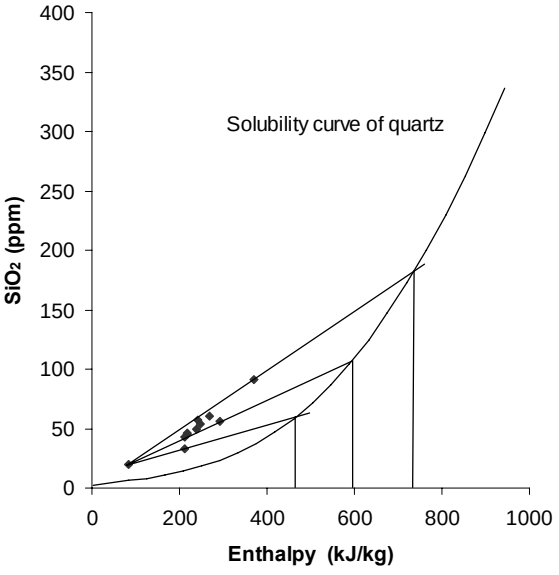

FIGURE 12: Dissolved silica-enthalpy diagram

1998, the drilling area has been expanded from the original 100 km^2 to other parts of the geothermal field, and the maximum well depth reached is 3,766 m. At present, there are 66 geothermal wells in use in the geothermal field, producing about 4 million m^3/a of 40-89°C geothermal water.

The long-term production of geothermal water has caused a remarkable lowering of the pressure in the geothermal reservoir, threatening the sustainability of geothermal exploitation. Therefore, strict measures have been taken to control the amount of geothermal water abstraction since 1985. As a result, the water level decline has slowed down (Figure 13). The production in the Urban field has an obvious periodicity. The space heating season in winter is from November to April, and then extraction increases and the water level drops. From June to October, extraction is decreased and the water level goes up again. The lowest water level of the year appears in April, while the highest one is in September. In recent years, the annual production from the Urban geothermal field has been around 4 million m^3.

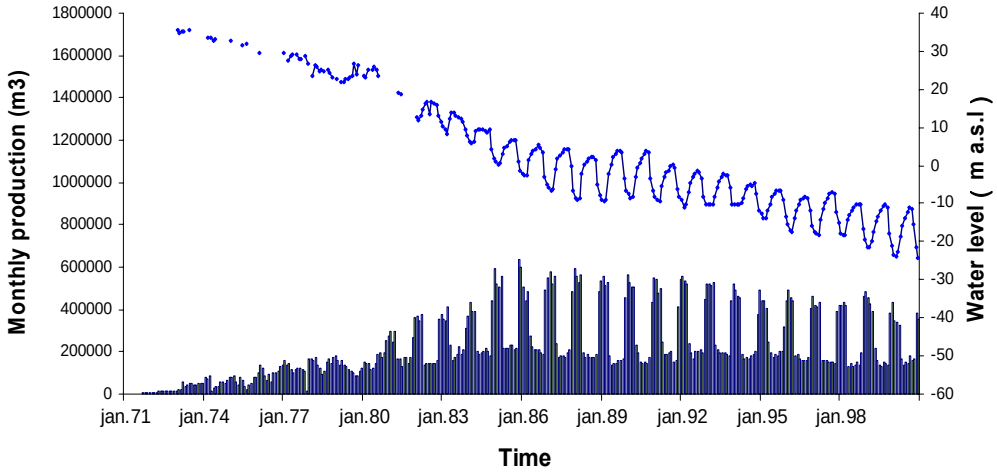

FIGURE 13: Changes in monthly production and water level in the Urban field

Monitoring the chemical changes of geothermal fluids from the production wells is very useful for estimating various kinds of changes in reservoir conditions (Chen, 2000). Well JR42, is located in the central part of the Urban field, near well JR35, with a depth of 2,071 m, and has been used for monitoring variations in water level since 1984. The chemical changes can be interpreted with reference to changes in the geothermal fluid utilized in the area. The chemical composition of water samples from JR42 during the period 1984 to 2000 is listed in Table 7.

The chemical composition has been studied as a function of time. The variations in concentrations of conservative components such as Cl, B, rock forming mineral constituents such as HCO_3, Mg, Ca, and geothermometer temperatures, can be useful in mapping the recharge into exploited geothermal reservoirs. The variations in certain components in well JR42 from 1984 to 2000 are plotted in Figure 14. The diagrams show the possible trend of changes in the reservoir during this period. The concentration of chloride (Cl) was 65.6 mg/l in 1984 and dropped to 45.2 mg/l in 1985, but no significant variation has been observed since. The concentration of bicarbonate (HCO_3) ranges from approximately 210 to 240 mg/l, and the value has been relatively stable except for a slight drop in 1991 but returned to previous values in 1992. The concentration of magnesium (Mg) ranges from 17.1 to 23.1 mg/l and no significant variation was observed except for the relatively low value observed in 1993. The concentration of calcium (Ca) has been stable during utilization. The concentration of HBO_2 shows minor changes in 1987 and 1993. Because of a lack of detailed wellhead temperature data, the chemical changes cannot be used to interpret temperature changes during exploitation. However, the calculated temperatures based on geothermometers can be used to study the temperature variations during this period. Quartz and K-Mg geothermometers were selected to calculate temperature in well JR42. The Tqc and Tkm vary a little during this monitoring period. But more

generally, according to Figure 14, most of the chemical composition of the geothermal water, as well as the average values were constant except for a slight singular deviations during these 17 years. The diagrams indicate stable recharge of thermal water and the good potential of the geothermal resource in the Urban field.

TABLE 7: Chemical composition of water samples from well JR42 (in ppm) in the Urban field, 1984-2000

Date	K	Na	Ca	Mg	HCO_3	SO_4	Cl	F	HBO_2	SiO_2	Fe	Al	NH_4	H_2S
1984-05-17	9.67	86.7	49.5	22.9	213.6	110.4	65.6	5.00	1.76	38.0	0.66	0.00	0.00	0.00
1985-03-25	10.12	79.3	45.8	21.4	231.9	115.8	45.2	3.65	2.24	33.0	2.40	0.00	0.00	0.29
1986-03-18	10.0	75.8	47.3	21.2	235.5	106.3	54.4	5.21	1.76	37.0	2.24	0.00	0.00	0.00
1987-03-20	9.2	77.4	45.6	21.9	238.0	101.8	53.6	5.16	3.12	34.0	1.68	0.00	0.00	0.12
1988-03-16	9.4	89.6	46.6	21.3	240.4	120.0	53.9	5.19	2.32	39.0	1.24	0.00	0.00	0.12
1989-03-29	10.7	80.2	45.5	21.2	244.1	106.1	52.3	4.79	1.20	35.0	1.08	0.00	0.00	0.08
1990-03-13	10.3	84.9	47.8	21.7	250.2	112.8	55.3	4.86	2.00	33.0	0.20	0.03	0.00	0.00
1991-03-16	10.2	84.0	44.0	20.8	244.1	103.9	53.3	5.50	2.20	36.0	0.12	-	0.00	0.13
1992-03-17	9.09	79.6	44.5	21.3	231.9	109.0	53.5	4.80	2.20	36.0	1.58	0.03	0.00	0.00
1993-03-17	9.27	82.4	42.7	17.1	244.1	107.2	51.5	5.40	0.40	35.0	1.41	0.01	0.03	-
1994-03-16	8.15	81.4	42.5	22.6	244.1	91.8	47.6	5.20	2.00	42.0	1.39	0.17	0.02	0.16
1995-03-14	9.01	82.6	43.4	22.2	244.1	106.9	52.9	5.40	2.00	40.0	2.18	0.02	0.08	0.08
1996-04-02	9.18	81.4	43.8	22.2	225.8	101.5	52.8	5.20	2.20	37.2	1.48	0.01	0.06	0.33
1997-03-27	8.80	86.5	40.5	22.5	238.0	108.3	49.7	5.00	2.00	39.3	2.00	0.09	0.03	0.38
1998-05-13	9.14	78.7	44.1	22.1	240.4	102.3	52.6	5.10	2.20	38.5	2.00	0.23	0.10	0.36
1999-04-05	8.74	83.3	44.1	21.9	240.4	92.3	54.5	5.10	1.80	36.5	2.60	0.75	0.05	0.00
2000-04-03	8.85	80.3	43.5	23.1	226.0	104.0	52.9	5.30	1.80	36.8	4.00	0.03	0.04	0.08

4.2 Utilization

Geothermal fluid from the Urban field is used for various direct purposes including space heating, domestic hot water (bathing, recreation and spas), fish farming, greenhouses and mineral water production (stopped recently) (see Table 8). The Summer Olympic Games of 2008 will be held in Beijing. The Olympic Green (Olympic Park), where the most important facilities for the great event are to be built, is in the northern part of the city on the edge of the Urban field (Chen et al., 2003). Geothermal energy will be used for space heating and bathing in the sports village that will be more than 29 ha in area (Liu et al., 2003).

TABLE 8: Geothermal water utilization in the Urban geothermal field (Liu et al., 2002)

Item	Bathing	Space heating	Chemical treatment	Mineral water production	Aquaculture	Total
Geothermal wells	33	12	1	1	1	48
Production ($10^3 \times m^3/a$)	2106	1489	112	77	200	3984
Share of production (%)	52.9	37.4	2.8	1.9	5.0	100

Space heating is the primary utilization of the Urban geothermal field (Table 8) besides bathing. The heated area has reached 240,000 m^2. With the enlarged heating pipeline from the thermoelectricity plant in recent years, the area of geothermal space heating has been reduced. There were 12 heating units utilizing geothermal energy in the period 1999 to 2000 and the production of geothermal water was 1,489,000 m^3, and the heating area 200,000 m^2. In the near future, space cooling will be a major requirement, especially in the summer, thus the use of an absorption chiller (if temperatures are above

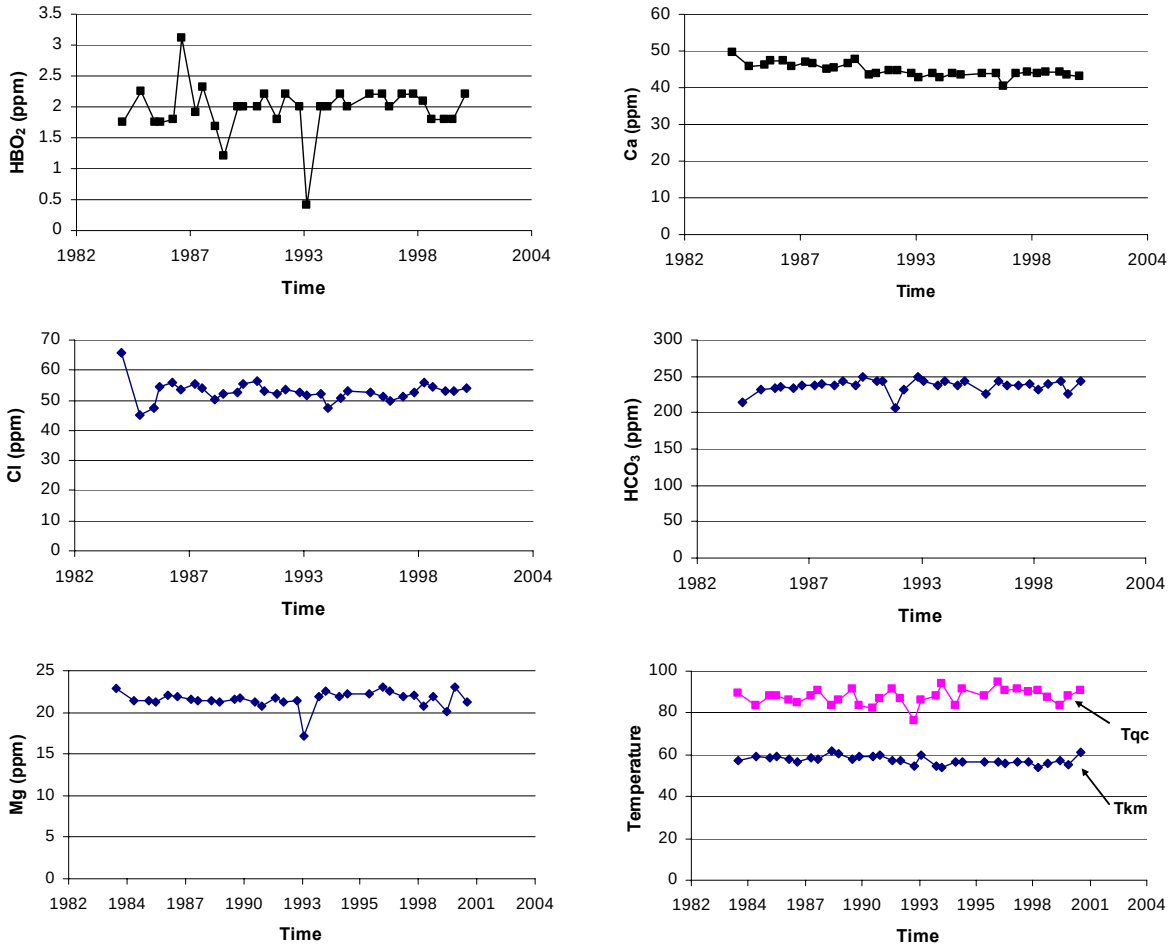

FIGURE 14: Variations of certain elements with time in well JR42 in the Urban field

90°C) and ground-source heat pumps should be considered (using ground-coupled or groundwater configurations at shallow depths).

Bathing: Hot spring water has been used for bathing and spas in Beijing for a very long time. Bathing is a popular geothermal utilization in the Urban area. There were 33 wells used for bathing in 1999 using a thermal water volume of 2,106,000 m^3, serving 92 thousand people per day.

Medical treatment: Geothermal water contains certain kinds of mineral components which at warm temperatures can effectively treat some diseases and be beneficial to health, associated with friendly atmosphere (Zheng 2004). Chinese medicine theory and actual results provide the best examples proving that geothermal water can cure or prevent many diseases such as chronic eczema, rheumarthritis and hypertension. The geothermal water has a broad application for medical treatments, mainly with three aims: to prevent diseases, to cure diseases and recuperation. The element Li in thermal water has a activation and detoxification function, and is used to contain cancer and treat mania; Sr, Se and Zn benefit the formation of bones and can prevent cardiovascular diseases and enhance eyesight; Br can restrain and adjust the central nerve system and the nerve activity of the pallium. In the Urban field, the geothermal water has a high trace element content. For example, the concentration of Sr is about 1 mg/l, Br is about 0.2 mg/l and B is 0.2-2.8 mg/l. Now people have realized the curative effects of the geothermal water and make better use of it.

In addition, geothermal energy in the Urban field is also being applied in other areas. One well is used for *aquaculture*, one for *mineral water production* and one is used to *clean* machine components.

Future plans for geothermal uses should consider the heating of domestic hot water and swimming pool water, with the long term goal of providing heat for these facilities.

4.3 Environmental benefits

Geothermal energy has special advantages over fossil fuel energy. It is already generally accepted as an environmentally benign energy source. Geothermal energy has enormous environmental advantages compared to conventional power sources: less and more easily controlled atmospheric emissions; readily maintainable groundwater quality and minimal amounts of waste.

The development of geothermal resources in the Urban field not only creates a considerable economic benefit but also provides a distinct environmental profit. According to a rough estimate, geothermal water production of 4 million m^3 annually effectively results in 329 million RMB (102 million RMB directly, 227 million RMB indirectly). It can reduce the emission of dust to the atmosphere by about 342 tons, harmful gas about 3,285 tons and reduce the discharge of ash by about 5,085 tons. It is important for improving the environment of Beijing city (Liu et al., 2001).

TABLE 9: Environmental benefit assessment of geothermal resources in the Urban field

Time (year)	Geothermal water production (10^3 m^3)	Quantity of heat available (10^{12} J)	Reduced raw coal (10^{14} tons)	Reduced exhaust emission (tons)	Reduced fly ash (tons)	Reduced ash (tons)
1999	4000	586	3.3	3240	334	5000
2020	13106	1921	10.9	10592	1090	16400

5. SUMMARY AND CONCLUSIONS

The production history of the Urban Geothermal Field in Beijing City spans more than 30 years. Data from the geochemistry study and monitoring of the geothermal field may give useful information on the nature of the reservoir.

Water samples from geothermal wells located in the Urban field supply the following information on the geothermal fluids:

- The geothermal water in most of the wells could be classified as bicarbonate-sodium-chloride type in a $Cl\text{-}SO_4\text{-}HCO_3$ triangle diagram and a Piper diagram.
- Stable isotope $\delta^{18}O$ and δD relationship proves that the thermal waters is of meteoric origin.
- Most of the geothermal water has a scaling potential, shown by the log (Q/K) diagrams, for calcite and chrysotile.
- For estimation of aquifer temperature of the wells, different geothermometers were used. The subsurface temperature is 51-104°C according to the chalcedony geothermometer of Fournier (1977), which is in agreement with measured temperatures and thus it is regarded as a suitable geothermometer for this field. There is a potential for developing the geothermal resources in the centre of the sedimentatary basin.
- From the silica mixing model, it was deduced that the thermal water in the Urban field may be mixed with cold groundwater.
- The thermal waters are classified as peripheral waters.
- The chemical properties of the thermal water in the reservoir have not changed significantly during exploitation from 1984 to 2000, but the water level has come down with the increase in production over these years.

ACKNOWLEDGEMENTS

I would like to thank Dr. Ingvar B. Fridleifsson and Mr. Lúdvík S. Georgsson for giving me this opportunity to participate in the UNU Geothermal Training Programme and to Mrs. Gudrún Bjarnadóttir for her careful help and kindness during this period. I sincerely thank my supervisor Dr. Halldór Ármannsson for his excellent guidance and generous help with my report during all stages of its preparation. I am also pleased to thank Dr. Liu Jiurong and Dr. Zhou Xun for their valuable assistance. This study is supported by the NSFC (National Natural Science Foundation of China) Earth Sciences Project. I convey my good wishes to the staff members at Orkustofnun and ÍSOR, especially the Geochemical Department for their constructive discussions.

Finally, I wish to give my deepest thanks to my parents and friends for their understanding and their spiritual support during the six-month training.

REFERENCES

Árnason, B., 1976: *Groundwater systems in Iceland traced by deuterium*. Soc. Sci. Islandica, 42, Reykjavík, 236 pp.

Arnórsson, S., 1975: Application of the silica geothermometer in low-temperature hydrothermal areas in Iceland. *Am. J. Sci., 275,* 763-783.

Arnórsson, S., 1985: The use of mixing models and chemical geothermometers for estimating underground temperature in geothermal systems. *J. Volc. Geotherm. Res., 23,* 299-335.

Arnórsson, S., 1991: Geochemistry and geothermal resources in Iceland, In: D´Amore, F. (co-ordinator), *Applications of geochemistry in geothermal reservoir development.* UNITAR/UNDP publication, Rome, 145-196.

Arnórsson, S., 2000: The quartz and Na/K geothermometers. I. New thermodynamic calibration. *Proceedings of the World Geothermal Congress 2000, Kyushu-Tohoku, Japan,* 929-934.

Arnórsson, S., Gunnlaugsson, E., and Svavarsson, H., 1983: The chemistry of geothermal waters in Iceland III. Chemical geothermometry in geothermal investigations. *Geochim. Cosmochim. Acta, 47*, 567-577.

Arnórsson, S., Sigurdsson, S., and Svavarsson, H., 1982: The chemistry of geothermal waters in Iceland I. Calculation of aqueous speciation from 0°C to 370°C. *Geochim. Cosmochim. Acta, 46,* 1513-1532.

Bin D., Liu Y., Bai T., Pan X., Zhang D., Wu M., Chen J., Jia H., Liu Z., and Yu X., 1999: *The geothermal development plan for the beginning of the 21st Century in the city of Beijing* (in Chinese). Beijing Bureau of Geology and Mineral Resources, Beijing, 44 pp.

Bjarnason, J.Ö., 1994: *The speciation program WATCH, version 2.1.* Orkustofnun, Reykjavík, 7 pp.

Chen J., Liu Q., Lu J., Feng H., Xu Y., Wu H., and Zhao L., 2003: *Report of geothermal resources explorations for the area of Olympic Green, Beijing*. Beijing Institute of Geotechnology, report (in Chinese).

Chen Z., 2000: Analyzing the long-term exploitation stability of Beijing geothermal field from geothermal water chemistry. *Proceedings of the World Geothermal Congress 2000, Kyushu-Tohoku, Japan,* 1053-1058.

Connolly, C., Walter, L., Baadsgaard, H., and Longstaff, F., 1990: Origin evolution of formation waters, Alberta Basin, Western Canada Sedimentary Basin, II. Isotope systematics and water mixing, *Applied Geochemistry, 5,* 397-413.

Craig, H., 1961: Isotopic variations in meteoric water. *Science, 133*, 1702-1703.

Fang T., and Zhu H., 2002: Tectonics and environment change of Meso-Cenozoic in China continent and its adjacent areas, *J. Geoscience,* 16-2, 107-120.

Fournier, R.O., 1977: Chemical geothermometers and mixing model for geothermal systems. *Geothermics, 5,* 41-50.

Fournier, R.O., 1979: Geochemical and hydrologic considerations and the use of enthalpy-chloride diagrams in the prediction of underground conditions in hot spring systems. *J. Volc. & Geoth. Res., 5,* 1-16.

Fournier, R.O., and Potter, R.W. II, 1982: A revised and expanded silica (quartz) geothermometer. *Geotherm. Resourc. Counc. Bull., 11-10,* 3-12.

Fournier, R.O., and Rowe, J.J., 1966: Estimation of underground temperatures from the silica contents of water from hot springs and wet steam wells. *Am. J. Sci., 264,* 685-697.

Fournier, R.O., and Truesdell, A.H., 1973: An empirical Na-K-Ca geothermometer for natural waters. *Geochim. Cosmochim. Acta*, *37*, 1255-1275.

Giggenbach, W.F., 1988: Geothermal solute equilibria. Derivation of Na-K-Mg-Ca geoindicators. *Geochim. Cosmochim. Acta, 52*, 2749-2765.

Giggenbach, W.F., 1991: Chemical techniques in geothermal exploration. In: D'Amore, F. (coordinator), *Application of geochemistry in geothermal reservoir development*. UNITAR/UNDP publication, Rome, 119-142.

Giggenbach, W.F., Gonfiantini, R., Jangi, B.L., and Truesdell, A.H., 1983: Isotopic and chemical composition of Parbati Valley geothermal discharges, NW-Himalaya, India. *Geothermics, 12*, 199-222.

Hitchon, B., and Friedman, I., 1969: Geochemistry and origin of formation waters in the western Canada sedimentary basin. I. Stable isotopes of oxygen and hydrogen, *Geochim.Cosmochim Acta, 33,* 1321-1349.

Huang S., 2000: Looking back and ahead for geothermal energy development in China. *Proceeding of the World Geothermal Conference 2000, Kyushu-Tohoku, Japan,* 1259-1264.

Liu J., Pan X., Yang Y., Liu Z., and Wang X., 2001: *Report of geothermal synthetic assessment for the Urban geothermal field in the City of Beijing*. Beijing Institute of Geological Engineering, China, report (in Chinese) 74 pp.

Liu J., Pan X., Yang Y., Liu Z., Wang X., Zhang L., and Xu W., 2002: Potential assessment of the Urban geothermal field, Beijing, China. *Proceedings of the 2002 Beijing International Geothermal Symposium*, Beijing, 211-217.

Liu J., Zheng K., Xu W., Liu Z., and Bin D., 2003: *Report of geothermal assessment for the Area of the Olympic Green,* Beijing Institute of Geological Engineering, report (in Chinese).

Nicholson, K., 1988: *Geochemistry of geothermal fluids: An introduction.* Geothermal Institute, University of Auckland, New Zealand, report, 87 pp.

Pang Z., 2000: Isotope geochemistry of geothermal waters in northern north China basin: implications on deep fluid migration*, Proceedings of the World Geothermal Congress 2000, Kyushu-Tohoku, Japan,*1559-1563

Stanasel, O., and Ludovic, G., 2003: Interpretation of geochemical data from wells in the western geothermal field of Romania. *Proceedings of the International Geothermal Conference, IGC2003, Reykjavik,* S04 1-7.

Tonani, F., 1980: Some remarks on the application of geochemical techniques in geothermal exploration. *Proceedings, Adv. Eur. Geoth. Res., 2nd Symposium, Strasbourg*, 428-443.

Truesdell, A.H., 1976: Summary of section III - geochemical techniques in exploration. *Proceedings of the 2nd U.N. Symposium on the Development and Use of Geothermal Resources, San Francisco, 1,* liii-lxxix.

Truesdell, A.H., 1991: Effects of physical processes on geothermal fluids. In: D'Amore, F. (coordinator), *Application of geochemistry in geothermal reservoir development.* UNITAR/UNDP publication, Rome, 71-92.

Yao Z., 2000: Environmental imprints on the temporal changes of the chemistry of geothermal water from some low-temperature geothermal fields in the north China plain. *Proceedings of the World Geothermal Congress 2000, Kyushu - Tohoku, Japan,* 1979-1984.

Zheng K., 2000: A study of water-rock equilibrium of low temperature geothermal reservoirs in China*, Proceedings of the World Geothermal Congress 2000, Kyushu-Tohoku, Japan,* 3009-3013.

Zheng K., 2004: Newest statistics of geothermal development in China. *Proceedings of the 6th Asian Geothermal Symposium*, *Daejeon, S-Korea,* 85-90.